Transport Simulations of KSTAR Advanced Tokamak Scenarios

Yong-Su Na 1), 2), C. E. Kessel 3), J. M. Park 4), J. Y. Kim 1)

1) National Fusion Research Institute, Daejeon, Korea
2) Department of Nuclear Engineering, Seoul National University, Seoul, Korea
3) Princeton Plasma Physics Laboratory, Princeton, NJ, USA
4) Oak Ridge National Laboratory, Oak Ridge, TN, USA

e-mail contact of main author: ysna@snu.ac.kr

Abstract. Predictive modeling of KSTAR operation scenarios are performed with the aim of developing high performance steady state operation scenarios. Various transport codes are employed for this study. Firstly, steady state operation capabilities are investigated with time dependent simulations using a free-boundary transport code. Secondly, reproducibility of high performance steady state operation scenario from an existing tokamak to KSTAR is investigated using the experimental data from other tokamak device. Finally, capability of DEMO-relevant advanced tokamak operation is investigated in KSTAR. From those simulations, it is found that KSTAR is able to establish high performance steady state operation scenarios. The selection of the transport model and the current ramp up scenario is also discussed which have strong influence on target profiles.

1. Introduction

As the fusion era is rapidly approaching, the necessity of development of steady state operation scenarios becomes more and more important, particularly for fusion reactor models based on the tokamak concept. In addition to the steady state operation, fusion performance of the tokamak needs to be improved compared with conventional H-modes for developing economically viable fusion power plants. In this context, the, so-called, advanced tokamak (AT) scenarios are being developed aiming at satisfying these two reactor requirements simultaneously.

The KSTAR (Korea Superconducting Tokamak Advanced Research) project has been launched in 1995 aiming at developing these AT scenarios. It is the first mission-oriented tokamak in the world for the AT scenario development. The research objectives of KSTAR are (i) to extend present stability and performance boundaries of tokamak operation through active control of profiles and transport, (ii) to explore methods to achieve steady state operation for tokamak fusion reactors using non-inductive current drive and (iii) to integrate high performance and steady state operation as a step toward an attractive tokamak fusion reactor [1]. The design feature of KSTAR is well-suited with the AT operation researches. The coil system of KSTAR is composed of superconducting toroidal and poloidal/central solenoid coils, allowing long pulse operation of 300 s at full heating power, about 30 MW. Plasma facing components are also designed to be capable of this 300 s operation. KSTAR has strong shaping capability, elongation of 2.0 and triangularity of 0.8 in double null configurations, which allows high MHD stability (high β_N). Moreover, installation of passive stabilizers close to the plasma improves the stability, resulting in increase of β_N up to 5. The heating systems consist of neutral beam injection (NBI) with 14 MW input power (2 beam boxes with 6 beam sources in each box at 120 keV in deuterium), ion cyclotron resonance frequency (ICRF) with 6 MW input power, electron cyclotron resonance frequency (ECRF) at 170 GHz with 5 MW input power and lower hybrid (LH) at 5 GHz with 3 MW.

In this paper, predictive modelling of AT scenarios is performed for the first half operation phase of KSTAR programme; NBI power of 7.4 MW, ICRF power of 3 MW, EC power of 3 MW and LH power of 3 MW. Firstly, steady state operation capabilities are investigated with time dependent simulations using a free-boundary transport code. Secondly, reproducibility of high performance steady state operation scenario from an existing tokamak to KSTAR is investigated using the experimental data from other tokamak device. Finally, capability of DEMO-relevant AT operation is investigated in KSTAR.

The paper organizes as following; the description of modeling tools is given in section 2.1. The capability of steady state operation of KSTAR is described in section 2.2. Section 2.3 presents the reproducibility of AT scenarios from an existing tokamak is presented in 2.3. The capability of DEMO-relevant AT operation is given in section 2.4 and effect of transport model selection is discussed in chapter 3. The paper finalized with summary and conclusions.

2. Predictive Modelling of Advanced Tokamak Scenarios

2.1. Description of modelling tools

The simulations are performed using several various transport codes; ASTRA [2], ONETWO [3] and TSC/TRANSP [4,5] where the plasma equilibrium, current diffusion, heating and current drive (CD) and transport are calculated self-consistently.

The ASTRA code solves coupled, time-dependent, 1-D transport equations for particles, heat, and current, as well as 2-D MHD fixed boundary equilibrium self-consistently with a realistic tokamak geometry. In this paper, up-down symmetry of the plasma configuration is assumed. For predictive transport modelling, the Weiland transport model [6] is employed. The neutral beam injection (NBI) package [7] is embedded in ASTRA for the calculation of NBI heating and CD. CURRAY [8] for ICRF, TORAY [9] (ray-tracing relativistic damping) for EC, and LSC (ray-tracing quasilinear 1D Fokker Planck) [10] for LH are used for simulations. The Hirshman [11] model is employed for plasma resistivity, the Sauter [12] model is used for bootstrap current, and the neoclassical ion and electron transport coefficients are from [13] and [14], respectively. The simulations include Bremsstrahlung, cyclotron and line radiation from Carbon.

The ONETWO transport code solves the flux surface averaged transport equations for energy, particles, toroidal rotation, current density and equilibrium evolution with self-consistent source and sink calculations. Predictive simulation from ONETWO is preformed with the GLF23 [15] transport model. The source models used in ONETWO are TORIC (full wave) [16] for ICRF, the Monte Carlo code, NUBEAM (Monte Carlo orbit following) [5] for NBI and LSC for LH. The bootstrap and plasma resistivity are taken from Sauter's model. Radiation includes Bremsstrahlung, cyclotron (assumed to be re-absorbed), and line from [17].

The Tokamak Simulation Code (TSC) is used for the TSC/TRANSP predictive free-boundary time-dependent transport simulations, and solves the axisymmetric 2-D MHD-Maxwell's equations on a rectangular grid. 1-D flux surface averaged transport equations are solved for energy, particles, and current density utilising predefined transport coefficients. TRANSP is used in the "interpretive" mode, where it receives equilibrium data, ion and electron temperature profiles, density profile, and Zeff profile from TSC, and solves flux conservation equations governing the flux surface averaged 1-D transport for energy, particles, current

density, and momentum employing the GLF23 transport model. The source deposition and current drive profiles from TRANSP are then fed back to TSC. The source models in TRANSP include NUBEAM for NBI, CURRAY for ICRF, TORAY for EC, and LSC for LH. TRANSP accounts for the fast particle distribution functions from NBI and fusion and includes them in the ICRF damping through equivalent Maxwellians derived from their slowing down distributions. The Sauter's bootstrap formulation, and the Hirshman plasma resistivity formulation are used. The radiated power includes Bremsstrahlung, cyclotron (Trubnikov) and the coronal equilibrium treatment for line.

2.2. Investigation of steady state operation capability of KSTAR in time dependent simulations

The fully non-inductive operation scenario is simulated with TSC/TRANSP. The simulation is performed for plasmas from the start up phase with 0.5 MW of ECRH at 84 GHz to the current flattop phase. Outboard start up scheme is employed and the plasma is diverted as early as possible to allow H-mode transition as well as slow current diffusion. Plasma current at the flattop phase is 1.05 MA and toroidal magnetic field is 2 T. The density profile is prescribed and Z_{eff} is assumed to be 2.0. NBI power of 5.4 MW, ICRF power of 3 MW and LH power of 1 MW are applied at the flattop phase. The time trace of heating powers is shown in FIG. 1 (top left). The time evolution of amount of total plasma current, bootstrap current, NBCD and LHCD is plotted in FIG. 1 (top right) together with amount of the total non-inductive (NI) current.

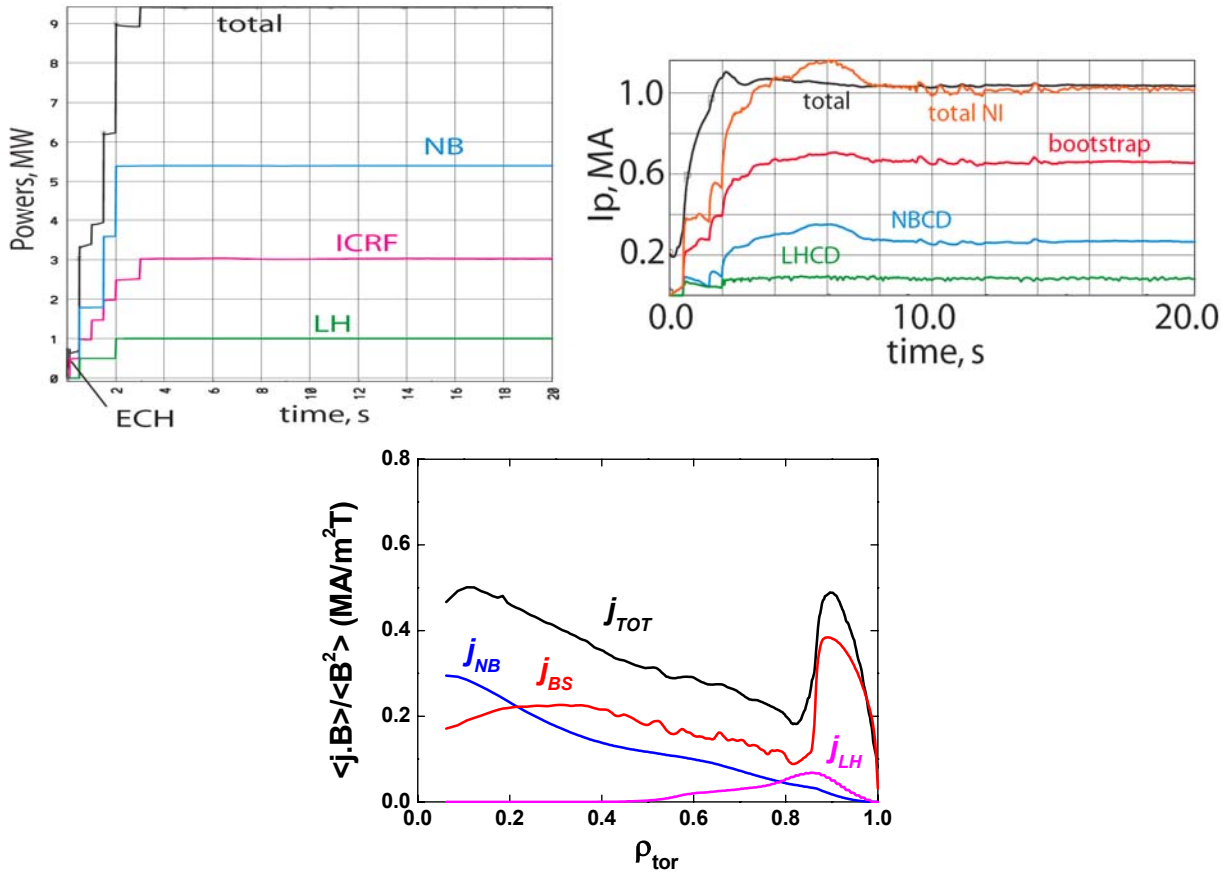

FIG. 1. Time trace of heating powers (top left), currents (top right) and current density profiles (bottom)

As shown, fully non-inductive current drive is able to be achieved in this simulation for the PF/CS coil system and heating and current drive system of the first half operation phase of KSTAR. The current density profiles are presented in FIG. 1 (bottom). Here, q(0) = 2.0 and q_{min} = 1.88 are obtained, accordingly expected to be stable against (3,2) neoclassical tearing mode (NTM). Fusion performance is improved in this simulation compared with standard H-modes; β_N = 2.65, $H_{98}(y,2)$ = 1.40 obtained in this simulation.

2.3. Investigation of advanced scenario reproducibility of KSTAR

A simulation is performed to investigate the reproducibility of advanced scenarios already established in other tokamak devices. Fully non-inductive AT scenario is selected from DIII-D. The ONETWO code employing the GLF23 transport model, which has been extensively validated against DIII-D AT discharges, is applied to KSTAR for the simulation. For example, FIG. 2 shows that the ONETWO simulation is in agreement with experimental measurements. Here, electron density profile is prescribed and temperature profiles are calculated with boundary conditions at ρ = 0.9.

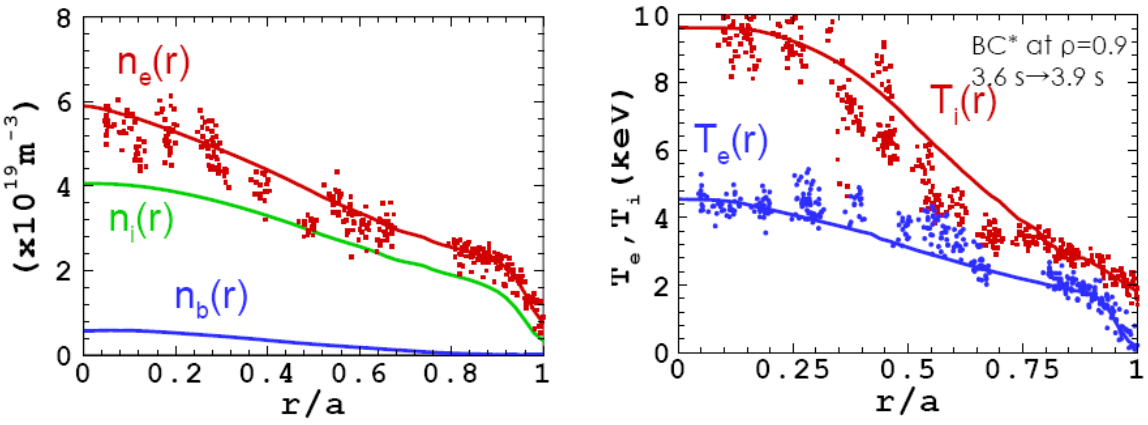

FIG. 2. ONETWO simulation results for DIII-D AT discharge.
Electron, ion and beam density profiles (left), Ion and electron temperature profiles (right)

Based on this DIII-D AT discharge, a predictive simulation is carried out with the density and the Z_{eff} profile and boundary conditions taken at a single time point. Plasma current is 1.0 MA and toroidal magnetic field is 2 T. NBI power of 5.4 MW, ICRF power of 3 MW (30 MHz minority heating) and LH power of 1 MW are applied. The current density profiles are plotted in FIG. 3 (left). The total plasma current density profile shows reversed shear configuration with a peak where maximal bootstrap current is located. In this simulation, fully non-inductive current drive is achieved with bootstrap current of 0.611 MA (61.1%), NBCD of 0.357 MA (35.7%) and LHCD of 0.114 MA (11.4%). The q-profile is shown in FIG. 3 (right) in magenta with q(0) = 2.83 and q_{min} = 1.52, which exhibits plasma is stable against (3,2) NTM. Electron and ion temperature profile and electron density profile are presented in FIG. 3 (right). It is likely that internal transport barriers are formed in both ion and electron channels which could drive high fusion performance with β_N = 3.76 and $H_{98}(y,2)$ = 2.0 as well as high bootstrap current.

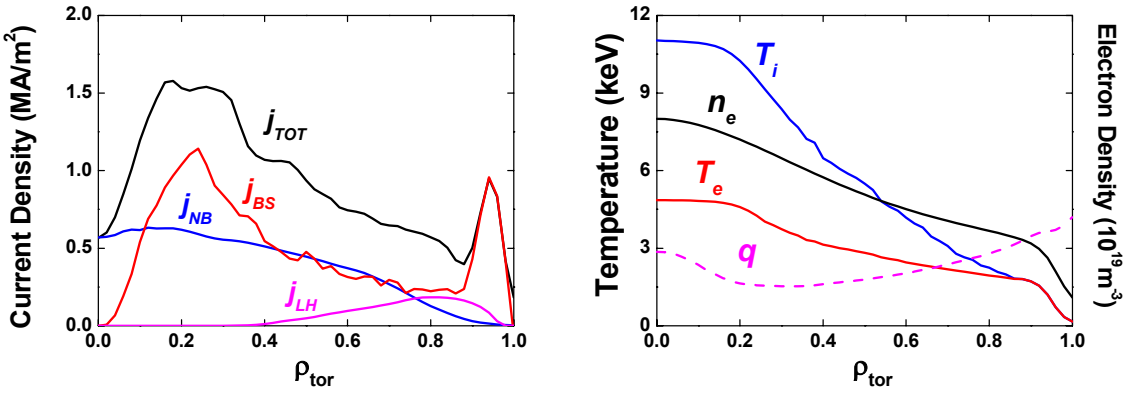

FIG. 3. Current density profiles (left), temperatures, density and q- profiles (right)

2.4. Investigation of DEMO-relevant advanced tokamak operation capability of KSTAR in time dependent simulation

As KSTAR is targeting to address DEMO-relevant issues, DEMO-relevant conditions are attempted to be realised in this simulation as follwing; fully non-inductive current drive with a bootstrap current fraction above 60%, high β_N above $4xl_i$, high volume averaged electron density above 60% of the Greenwald density, low plasma rotation, $T_e \sim T_i$ and q_{min} above 2 to avoid the (2,1) NTM activity. The time dependent simulation is performed with ASTRA. The density profile is prescribed in the entire simulation with $<n_e>/n_{GW} = 0.6$ and the density peaking factor $n_e(0)/<n_e> \sim 1.5$. Here, the peaking factor is selected which satisfies the relation between $n_e(0)/<ne>$ and ν_{eff} for KSTAR conditions as shown in FIG. 4 [18].

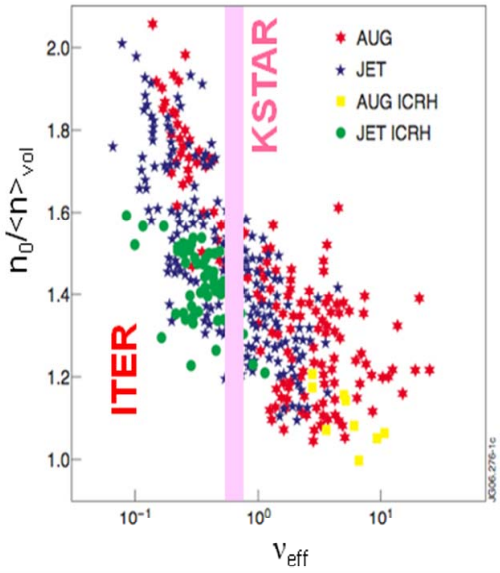

FIG. 4. Density peaking factor versus collisionality for KSTAR

The time dependent simulation is started at 0.7 s. Plasma current is 0.8 MA and toroidal magnetic field is 1.95 T at the current flattop phase. Z_{eff} is assumed to be 2.0. The current flattop phase is reached at 2 s considering superconducting magnet coil restrictions. NBI

power of 5.4 MW and LH power of 3 MW are applied in the flattop phase. The time trace of heating powers is presented in FIG. 5. When the current flattop phase is reached, NB heating power of 2.7 MW and LHCD power of 2 MW are added which results in considerable increase of the total non-inductive current drive fraction. Here, the two NB sources are balanced to establish a low rotating plasma condition, resulting in nearly zero beam driven current.

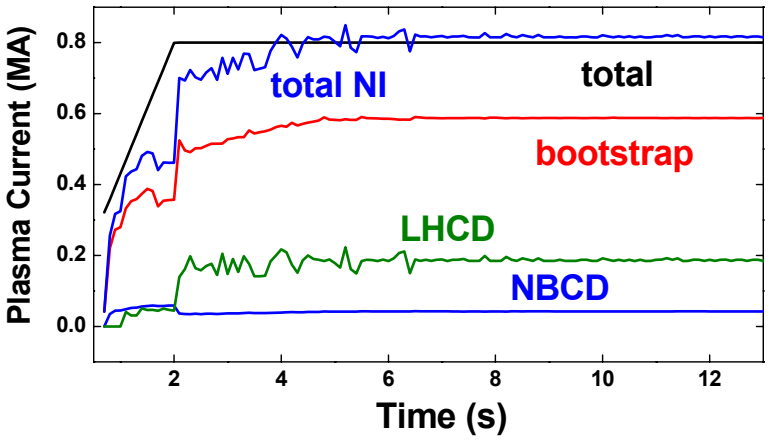

FIG. 5. Time trace of total and total non-inductive current, bootstrap current, LH and NB driven current

The current density profiles at 12 s are plotted in FIG. 6 (left). The total plasma current density profile shows a reversed shear configuration with a peak where maximal LH current is driven. Fully non-inductive current drive is achieved with bootstrap current of 0.587 MA (73.4%), NBCD of 0.042 MA (5.3%) and LHCD of 0.188 MA (23.5%). Here, it is worthy to note that the balanced NBI gives rise to slightly negative current drive at the centre of the plasma. The reason is unknown yet. The q-profile is shown in FIG. 6 (right) in magenta with q(0) = 12.36 and q_{min} = 3.04, which exhibits plasma is stable against the (2,1) NTM activity. Temperatures, electron density profile at 12 s are presented in FIG. 6 (right). Electron temperature is slightly higher than ion temperature although their boundary conditions around the pedestal region are the same. β_N is 3.16 above 4xli(3) = 1.84 and H_{98}(y,2) = 1.71.

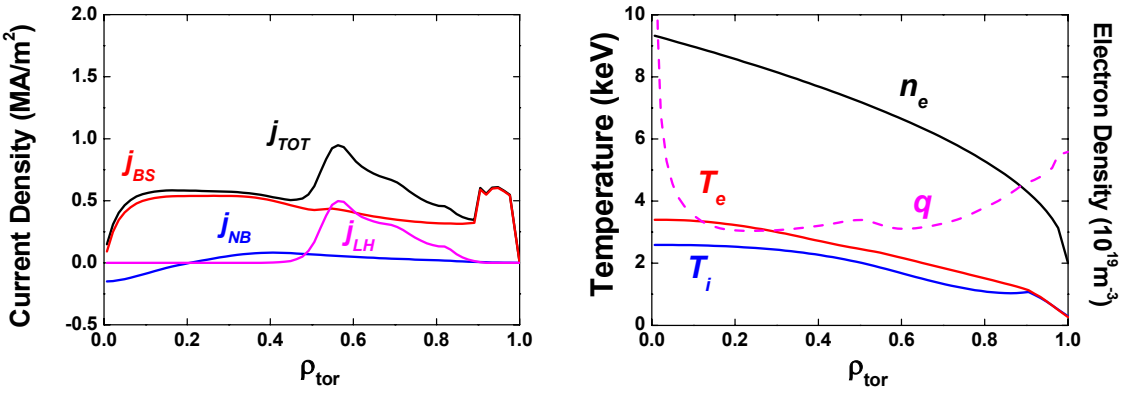

FIG.6. Current density profiles (left), temperatures, density and q- profiles at 12 s (right)

3. Discussions

3.1. Effect of the transport model

To investigate the effect of transport model selection, simulations are performed with different transport models but in same simulation settings for a DEMO-relevant operation mode. The results are compared in FIG. 7. As shown, all the results exhibit different temperature profiles. The Weiland model presents the most optimistic result, however the GLF23 model rather pessimistic one. The IFS/PPPL model stays more or less in between. As temperature profiles become different, plasma performance as well as q(0), q_{min} and non-inductive current drive fraction become different. Fully non-inductive current drive cannot be achieved in the GLF23 and the IFS/PPPL cases.

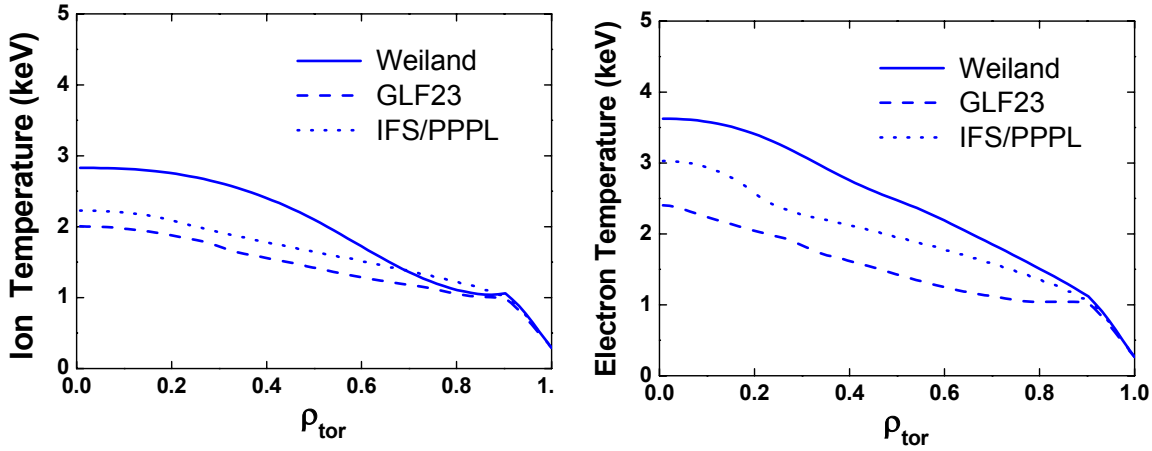

FIG.7. Comparison of ion and electron temperature profiles with different transport models

3.1. Effect of the current ramp up scenario

In real experiments, it is necessary to develop optimal current ramp up scenarios to achieve a reversed shear profiles. Generally, recipes to heat up the plasma by external heating or current drive sources in the current ramp up phase with fast current ramp up rates are being used. The DEMO-relevant scenario presented in section 2.4 follows this recipe except the current ramp up rate due to superconducting magnet coil restrictions. In order to investigate the effect of current ramp up scenario, a simulation is carried out which starts at 5 s without considering the current ramp up phase and compared with the result shown in section 2.4 both at 12 s. All simulation settings such as the density profile, heating power, etc. are the same between the two cases. The initial q-profile is also the same. As presented in FIG. 8, different plasma profiles are observed. Temperatures are increased resulting in slightly higher β_N of 3.18, however LHCD is rather decreased to 0.122 MA resulting in lower non-inductive current drive fraction of 92.7%. The q-profile is also observed to be different as q(0) = 4.94 and q_{min} = 2.19. Therefore, it is clarified that the current ramp up scenario is very important to establish optimal target profiles particularly in AT scenarios.

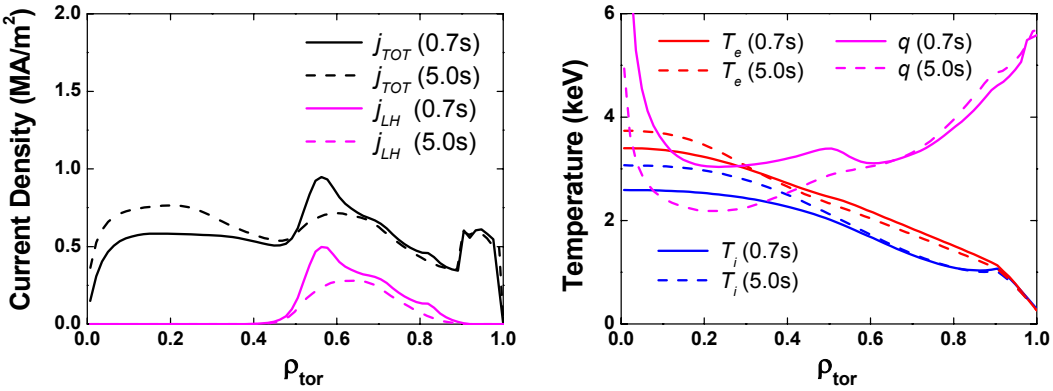

FIG.8. Current density profiles (left), temperatures and q- profiles at 12 s (right)

4. Summary and Conclusions

It is found by predictive transport simulations that i) fully non-inductive steady state operations are feasible in KSTAR with the PF/CS coil system and heating and current drive systems currently planned, ii) fully non-inductive with high performance scenario from an existing tokamak device (DIII-D) can be reproduced in KSTAR and iii) DEMO-relevant AT operation could be possible in the first half operation phase of KSTAR programme. It should be pointed out that the simulation result is very sensitive to selection of the transport model and the current ramp up scenario. Therefore, it could be desirable to verify developed target profiles with various transport models and current ramp up scenarios.

References

[1] Lee G S *et al* 2000 *Nucl. Fusion* **40** 575
[2] Pereverzev G *et al* 2002 IPP-Report IPP 5/98
[3] St. John H E *et al* Plasma Physics and Controlled Nuclear Fusion Research 1994, in *Proceedings of the 15th IAEA Conference,* Seville, IAEA, Vienna, 1994, Vol. 3, p. 603
[4] Jardin S C *et al J. Comput. Phys.* **66** 481
[5] Goldston R J *et al J. Comput. Phys.* **43** 61
[6] Weiland J *et al* 1989 *Nucl. Fusion* **29** 1810
[7] Polevoi A *et al* 1997 JAERI-Data/Code 97-014
[8] Mau T K *et al* Radio Frequency Power in Plasmas: 12th Topical Conference, edited by Ryan/Intrator, AIP, 1997, pp. 243-246
[9] Kritz A H *et al* Heating in Toroidal Plasmas 1982, in *Proceedings of the 3rd Joint Varenna-Grenoble Int. Symp. Grenoble*, Brussels, 1982, Vol. 2 CEC, p. 707
[10] Ignat D W *et al* 1994 *Nucl. Fusion* **34** 837
[11] Hirshman S P *et al* 1977 *Nucl. Fusion* **17** 611
[12] Sauter O *et al* 1999 Phys. Plas. **6** 2834
[13] Galeev A A and Sagdeev R Z 1973 *Voprosy Teorii Plasmy* **7** 210
[14] Angioni C and Sauter O 2000 *Phys. Plasmas* **7** 1224
[15] Waltz R E *et al* 1997 *Phys. Plasmas* **4** 2482
[16] Brambilla M 1996 A Full Wave Code for Ion Cyclotron Waves in Toroidal Plasmas, Rep. IPP 5/66, Max-Planck-Institut fur Plasmaphysik, Garching
[17] PPPL-1352.
[18] Weisen H 21st IAEA Fusion Energy Conference, , Chengdu, China, 2006, EX8-4